Proc. Natl. Acad. Sci. USA
Vol. 93, pp. 479–484, January 1996
Medical Sciences

Gain of chromosome 3q defines the transition from severe dysplasia to invasive carcinoma of the uterine cervix

KERSTIN HESELMEYER*†, EVELIN SCHRÖCK*, STANISLAS DU MANOIR*, HARALD BLEGEN†, KEERTI SHAH‡, RÜDIGER STEINBECK§, GERT AUER†, AND THOMAS RIED*¶

*Diagnostic Development Branch, National Center for Human Genome Research/National Institutes of Health, Building 49, Room 4A28, 49 Convent Drive, MSC 4470, Bethesda, MD 20892; †Department of Pathology, Karolinska Institute and Hospital, Stockholm, Sweden; ‡Johns Hopkins University School of Hygiene and Public Health, Baltimore, MD 21205; and §Institute of Pathology, Flensburg, Germany

Communicated by Michael Potter, National Cancer Institute, Bethesda, MD, October 20, 1995 (received for review July 3, 1995)

ABSTRACT **We have chosen tumors of the uterine cervix as a model system to identify chromosomal aberrations that occur during carcinogenesis. A phenotype/genotype correlation was established in defined regions of archived, formalin-fixed, and hematoxylin/eosin-stained tissue sections that were dissected from normal cervical epithelium ($n = 3$), from mild ($n = 4$), moderate ($n = 6$), and severe dysplasias/carcinomas *in situ* (CIS) ($n = 13$), and from invasive carcinomas ($n = 10$) and investigated by comparative genomic hybridization. The same tissues were analyzed for DNA ploidy, proliferative activity, and the presence of human papillomavirus (HPV) sequences. The results show that an increase in proliferative activity and tetraploidization had occurred already in mildly dysplastic lesions. No recurrent chromosomal aberrations were observed in DNA extracted from normal epithelium or from mild and moderate dysplasias, indicating that the tetraploidization precedes the loss or gain of specific chromosomes. A gain of chromosome 3q became visible in one of the severe dysplasias/CIS. Notably, chromosome 3q was overrepresented in 90% of the carcinomas and was also found to have undergone a high-level copy-number increase (amplification). We therefore conclude that the gain of chromosome 3q that occurs in HPV16-infected, aneuploid cells represents a pivotal genetic aberration at the transition from severe dysplasia/CIS to invasive cervical carcinoma.**

The multistep nature of carcinogenesis is firmly established (1–4). The sequence of genetic aberrations can be studied best in organs in which a histomorphological phenotype is defined for certain stages of tumor progression—e.g., colon cancer (5) and cancer of the uterine cervix. Regarding carcinomas of the cervix, infection with human papillomavirus (HPV) is known to play a crucial role in the immortalization of epithelial cells (6, 7). However, the persistence of HPV infection in women that do not develop dysplasias or carcinomas (8) and the long latency of the transition from severe dysplasia/carcinoma *in situ* (CIS) to carcinoma strongly suggest that factors in addition to HPV infection are required for the malignant transformation of epithelial cells (9). In analogy to colon carcinogenesis, mutations affecting tumor-suppressor genes or cellular oncogenes are likely candidates for additional "hits." Cytogenetically, those mutations are often present as specific chromosomal aberrations. However, relatively little is known about tumor-specific recurrent chromosomal aberrations in dysplastic lesions and primary invasive carcinomas of the uterine cervix—the second most frequent carcinoma in women worldwide—despite the fact that the importance of chromosomal aberrations in cervical carcinogenesis was recognized some 25 years ago (10). However, to date no landmark aberrations have been identified in cervical carcinomas (11, 12).

The scarcity of data on recurrent chromosomal aberrations that occur during the initiation and progression of cervical tumors prompted us to screen tissue from defined stages of cervical tumorigenesis by a molecular cytogenetic approach termed comparative genomic hybridization (CGH) (13, 14). CGH serves as a screening test for DNA copy-number changes in tumor genomes. CGH is based on a two-color fluorescence *in situ* hybridization, where a normal reference genome is labeled with a first fluorochrome (e.g., rhodamine) and genomic tumor DNA with a second fluorochrome (e.g., fluorescein). After hybridization of the differentially labeled genomes to normal reference metaphase chromosomes, changes in the ratio of the fluorescein/rhodamine intensities reflect DNA copy-number alterations in the tumor. Notably, genomic DNA is the only material from the tumor required for CGH analysis, thus allowing the use of archived, formalin-fixed, and paraffin-embedded samples as well (15). In the present study we have used this unique feature of CGH to demonstrate the potential of the technique to create a phenotype/genotype correlation during the genesis of cervical neoplasias. Tumor DNA was extracted from microdissected regions of histological preparations that were diagnosed on consecutive hematoxylin/eosin (HE)-stained sections. The same areas were analyzed for DNA ploidy, proliferative activity, and the presence of HPV genomes. The combined data provide a model for cervical carcinogenesis.

MATERIALS AND METHODS

Tissue Samples. The tumor material was collected between 1990 and 1994 from cervical biopsies or hysterectomies and diagnosed on HE-stained tissue sections at the Institute of Pathology, Flensburg, Germany, according to the World Health Organization classification (16). From each specimen eight contiguous sections were prepared and used for histological diagnosis (thickness; 4 μm), immunohistochemistry (4 μm), DNA ploidy measurements (8 μm), and microdissection (two sections, 50 μm). Before and after each 50-μm sample, 4-μm sections were cut for HE staining. All data were obtained from the dissected areas.

DNA Cytometry. DNA content measurements were performed by image cytometry of histological sections as described (17, 18). All DNA values were expressed in relation to the corresponding staining controls, which were given the value 2*c*, denoting the normal diploid DNA content, and are presented in such relative units. The specimens were divided into three main groups: (*i*) diploid cases with a distinct peak in the normal 2*c* region and no cells exceeding 5*c*, (*ii*) tetraploid cases with values in the 4*c* region and no cells or only a minor fraction of cells (<5%) exceeding 5*c*, and (*iii*) aneuploid cases with a main peak around the 4*c* region and varying numbers

The publication costs of this article were defrayed in part by page charge payment. This article must therefore be hereby marked "*advertisement*" in accordance with 18 U.S.C. §1734 solely to indicate this fact.

Abbreviations: CGH, comparative genomic hybridization; CIS, carcinoma(s) *in situ*; DAPI, 4′,6-diamidino-2-phenylindole; HE, hematoxylin/eosin; HPV, human papilloma virus.
¶To whom reprint requests should be addressed.

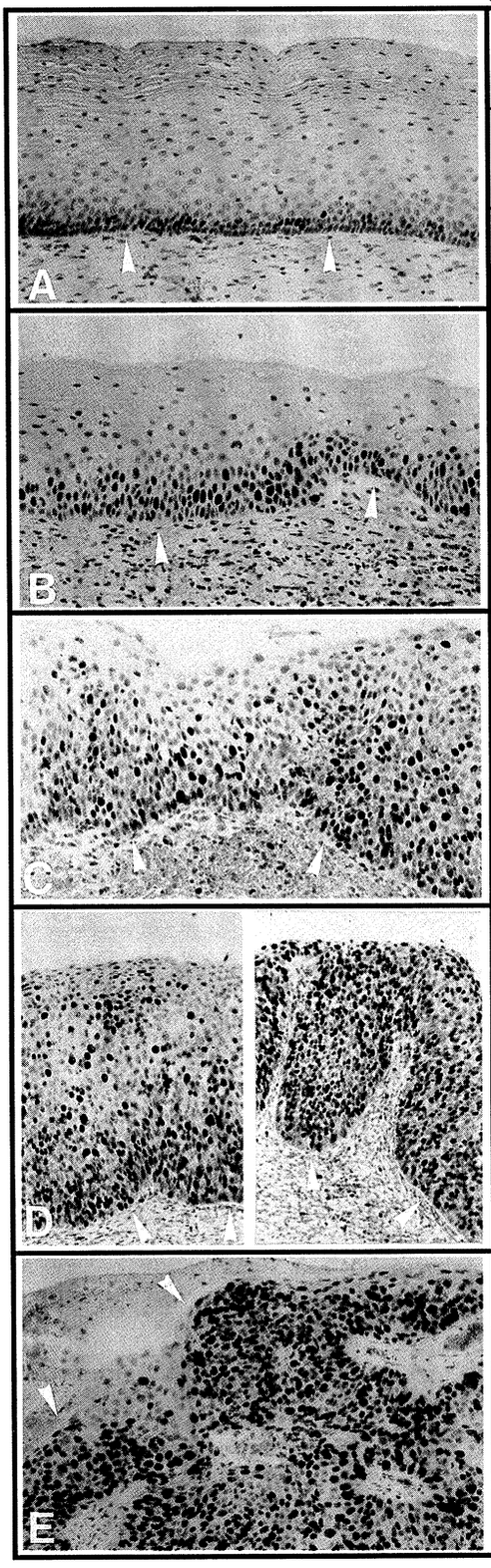

Case#	MIB (%)	DNA-Ploidy	HPV	CGH
1	10	2.0c, D	neg.	/
2	5	2.0c, D	neg.	/
3	10	2.0c, D	neg.	/
1	10	3.9c, T	n.d.	+18p,-X
2	15	3.8c, T	neg.	/
3	10	3.8c, T	n.d.	-X
4	20	4.1c, T	neg.	-X
1	40	4.7c, A	n.d.	+18p
2	n.d.	4.1c, T	neg.	/
3	30	4.1c, T	n.d.	/
4	n.d.	4.3c, A	neg.	-X
5	40	4.1c, T	n.d.	-X
6	30	4.3c, T	58	/
1	90	3.8c, A	16	/
2	85	3.8c, T	16	/
3	50	4.4c, T	n.d.	/
4	90	4.0c, A	16	/
5	80	5.0c, A	58	/
6	85	3.6c, A	33	-X
7	80	4.1c, A	16	/
8	90	4.1c, A	33	/
9	n.d.	3.6c, A	58	-X
10	n.d.	3.8c, T	16	/
11	80	3.9c, A	generic	+18p
12	90	3.7c, A	16	+3q,-3p22-24
13	n.d.	4.0c, T	16	/
1	90	4.8c, A	16	+3q,-4q,-13q21-qter
2	95	5.0c, A	45	+1q,+2p,+3q22-qter, +6p,-6q,+9q,-11p
3	90	4.2c, A	16	+3q,-13q21,-Xp
4	50	4.0c, T	18	/
5	85	5.0c, A	16	+3q,+5p,-3p,-6q, -X
6	80	4.0c, A	generic	+3q,-10,-11q14-qter
7	90	3.9c, A	16	+3q,-4q22-qter,-5q15-22
8	80	4.1c, A	16	+1,+3,+7,+9,+15,+17, +19,+21,+22
9	70	3.5c, A	31	+3q25-27,-3p,-X
10	75	4.4c, A	neg.	+3q,-X

FIG. 1. Summary of the results from MIB-1 staining, DNA ploidy measurements, HPV genotyping, and CGH in cervical epithelial cells from normal cervical epithelium ($n = 3$) (*A*), mild dysplasias ($n = 4$) (*B*), moderate dysplasias ($n = 6$) (*C*), severe dysplasias/CIS ($n = 13$) (*D*), and invasive carcinomas ($n = 10$) (*E*). Photographs (*Left*) represent examples of staining patterns after incubation with the antibody MIB-1. Arrowheads indicate the region that was dissected from the slide. MIB-1 staining results are also presented as percentages of the cells that reacted with the antibody [MIB-1 (%)]. The nuclear DNA content in the tissue sections is presented in indices, with 2*c* reflecting normal diploid DNA content (DNA ploidy); the histograms were classified as diploid (D), tetraploid (T), and aneuploid (A) (see also Fig. 2). The HPV-types are provided as determined by dot blot analysis (HPV); neg., no detection of HPV sequences; n.d., not determined. The CGH column shows the chromosomal aberrations detected in individual cases.

of cells (>5%) exceeding 5*c*. Examples of the histograms are presented in Fig. 2.

Immunohistochemistry. The monoclonal antibody MIB-1 (Immunotech) diluted 1:150 in 1% (wt/vol) bovine serum albumin and visualized with the routine avidin–biotin-peroxidase complex technique, was used for the detection of the Ki-67 antigen on 4-μm-thick tissue sections (17). The antibody discriminates nonproliferating (G_0) cells from proliferating ($G_1/S/G_2/M$) cells. Any distinct nuclear MIB-1 staining was recorded as positive. Examples of the staining pattern and a quantification of the results are shown in Fig. 1.

HPV Genotyping. HPV genomes in the purified specimen DNA were identified by PCR using the MY09–MY11 L1 consensus primers for amplification (19). Twenty-five type-specific probes and a generic HPV probe were used to diagnose the HPV type in the PCR products, as described in detail elsewhere (8).

CGH. Normal control DNA was prepared from peripheral blood lymphocytes of a cytogenetically normal male. Formalin-fixed, deparaffinized, and microdissected samples were provided in 50-μm-thick tissue pieces stored in 95% ethanol. DNA preparation, labeling, and hybridization were performed as described in detail elsewhere (20). In brief, 200 ng of digoxigenin-labeled normal DNA and 200 ng of biotin-labeled tumor DNA were hybridized for 4 days and detected with fluorescein conjugated to avidin (Vector Laboratories) and anti-digoxigenin Fab fragments conjugated to rhodamine (Boehringer Mannheim). Chromosomes were counterstained with 4′,6-diamidino-2-phenylindole (DAPI) and embedded in an antifading agent to reduce photobleaching.

Microscopy and Digital Image Analysis. Gray-level images were acquired with a cooled charge-coupled device (CCD) camera (Photometrics, Tucson, AZ) coupled to a Leica DMRBE epifluorescence microscope. Chromosomes were identified by DAPI banding. Fluorescence ratio images were calculated as described and the ratio profiles of individual reference chromosomes were determined by a custom computer program (21) and run on a Macintosh Quadra 950.

RESULTS

CGH was used to study the sequence of chromosomal aberrations that occur during the genesis of cervical carcinomas. Tumor DNA was extracted from distinct regions of histologically diagnosed cervical lesions. Specimens were dissected from normal cervical epithelium, from mild, moderate, and severe dysplasias/CIS, and from invasive carcinomas. All invasive tumors were diagnosed as stage T1. The cellular DNA content was assessed for all samples by image cytometry on Feulgen-stained tissue sections. A monoclonal antibody (MIB-1) directed against the Ki-67 antigen was used to monitor proliferative activity in the cells present in the dissected areas. HPV genotyping was performed on the DNA used for CGH by consensus-primer PCR and type-specific dot blot hybridization. Fig. 1 summarizes the results.

Normal Epithelium and Mild and Moderate Dysplasias. DNA was extracted from microdissected tissue of histomorphologically defined regions on consecutive sections of HE-stained slides of 13 samples: normal epithelium ($n = 3$), mild dysplasia ($n = 4$), and moderate dysplasia ($n = 6$). None of the DNA extracted from the normal mucosa and none of the two successfully tested mild dysplasias revealed the presence of HPV sequences, whereas one of the three successfully tested moderate dysplasias showed HPV58 sequences. The percentage of cells that stained positively with the proliferation marker MIB-1 was 5–10% in normal epithelium, 10–20% in mild dysplasia, and 30–40% in moderate dysplasia. The cells in the normal cervical epithelium revealed a diploid DNA distribution (Fig. 2*A*). A peak fraction at 4*c* was visible in the majority of the tissues diagnosed as mild and moderate dysplasias. A representative DNA histogram (mild dysplasia, case 3) is shown in Fig. 2*B*. Except for the loss of the X chromosome, CGH did not reveal any recurrent copy-number changes. One case of mild dysplasia and one case of moderate dysplasia showed a gain of the short arm of chromosome 18. See Fig. 1 for a summary of the results.

Severe Dysplasia/CIS and Invasive Carcinoma. PCR analysis of DNA extracted from severe dysplasias/CIS and carcinomas revealed invariably the presence of HPV genomes that are associated with cervical cancer—i.e., HPV types 16, 31, 33, 45, and 58. Immunoreactivity with MIB-1 was detected in 50–95% of the cells of severe dysplasia/CIS and carcinoma, reflecting high proliferative activity. The tetraploid cell population that prevailed in the mild and moderate dysplasias shifted increasingly to aneuploid cell populations, with scattered DNA values up to 8*c*, indicating pronounced genetic instability in severe dysplasias/CIS and invasive carcinomas. An example of an aneuploid DNA histogram is presented in Fig. 2*C*. The results are summarized in Fig. 1. The CGH analysis of DNA extracted from severe dysplasias/CIS revealed only a few specific chromosomal aberrations. In one case, loss of chromosome 3p was accompanied by a gain of chromosome 3q. As an example of the CGH analysis of a carcinoma (case 3) the ratio image with the respective average ratio profile is shown in Fig. 3. Average ratio profiles were used for the identification of chromosomal imbalances in all cases analyzed in this study. The karyogram of chromosomal gains and losses of 10 cases of carcinomas of the uterine cervix is displayed in Fig. 4. The number of chromosomal aberrations detected in invasive carcinomas by CGH was significantly higher compared with severe dysplasias/CIS. Losses of chromosomes or chromosomal subregions were observed in decreasing frequency on chromosomes X, 3p, 4q, 6, 11, and 13q. In 2 of 10 cases a gain of chromosomes 1q and 9q was observed. The most consistent finding in invasive cervical carcinomas was a gain of chromosome 3q, detectable in 9 of 10 cases. Notably, the gain of 3q was also observed as a high-level copy-number increase (amplification) in 3 cases. In 2 cases the ratio profile indicated a high-level copy-number increase for only a portion of 3q. The smallest region of overlap that was gained extended from chromosomal band 3q24 to band 3q28 (Fig. 4).

DISCUSSION

To study chromosomal imbalances during the genesis of cervical tumors, we used CGH to examine the DNA extracted from histomorphologically defined regions of formalin-fixed tissue sections. Proliferative activity and crude DNA ploidy were investigated in the same areas that were used for CGH. Additionally, HPV genotyping of the extracted DNA was performed by PCR and type-specific dot blot hybridization.

Our results indicate that the gain of chromosome 3q is the most consistent chromosomal aberration in cervical carcinomas and was present in 9 of 10 tumors. To our knowledge, this is the first study that has reported the recurrent gain of chromosome 3q in carcinomas of the uterine cervix. This aberration occurs during the progression from severe dysplasia/CIS to invasive carcinoma (stage T1), since only 1 of 13 severe dysplasias/CIS studied here showed an increase on 3q. The biological relevance of copy-number increases on this chromosomal region in carcinomas is further underlined by the fact that high-level copy-number increases (amplifications) were found on 3q as well.

Chromosomal losses were found less frequently in our collection of cervical carcinomas: in 3 of 10 cases chromosomes 3p and 4q were present in lower copy numbers. Studies for loss of heterozygosity implicate that regions on chromosome 3p and 11q are lost in primary tumors and cell lines established therefrom (22–25). In one of the carcinomas studied in our series, 11q was subject to loss as well. Notably, the loss of 13q and 17p, the chromosomal arms that harbor the retinoblas-

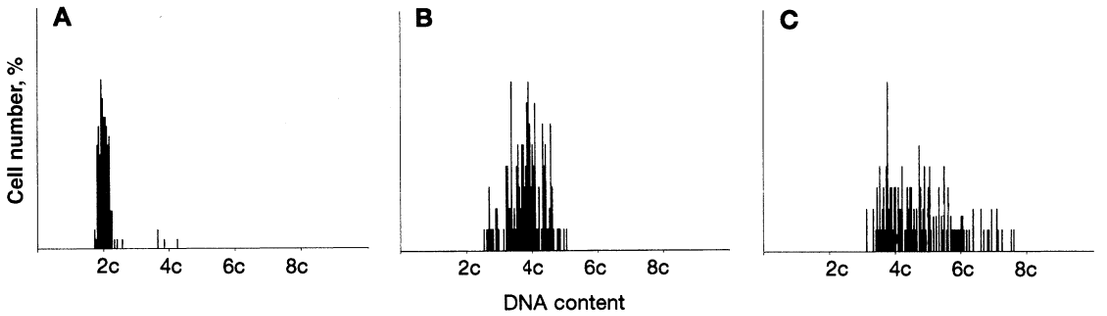

FIG. 2. DNA histograms displaying representative DNA values in the diploid range (*A*) or tetraploid range (*B*) and a scattered DNA histogram with values exceeding 5*C* (*C*). See *Materials and Methods* for details of the classification.

toma (RB) and p53 tumor-suppressor genes, is rare in cervical carcinomas. This is in significant contrast to findings in other tumors, such as breast and lung cancers, studied by CGH (20, 26). The discrepancy can be explained by the presence of HPV16 (or other high-risk HPV types) in virtually all cases of carcinomas analyzed in this study. HPV16 infection renders the cell p53-deficient and RB-deficient by complex formation of the viral proteins E6 and E7 with the products of these tumor-suppressor genes (27, 28). A regional copy-number decrease at the chromosomal map position of the RB tumor-suppressor gene (13q21) was observed in carcinoma cases 1 and 3. However, HPV16 was present in the DNA extracted from both tumors, indicating that infection with HPV16 and deletion of the RB tumor-suppressor gene are not mutually exclusive.

The karyogram of chromosomal gains and losses in cervical carcinomas (Fig. 4) is remarkable in two aspects. (*i*) The number of chromosomal aberrations is relatively low; only 17 chromosomes are involved in gains or losses, with an average number of 4.0 chromosomal aberrations per tumor. A significantly higher number of chromosomal aberrations was found in small-cell lung cancers (23 chromosomes involved; average number of aberrations, 13.0 per tumor), glioblastomas (23; 9.2), and aneuploid breast cancers (19; 6.8) analyzed in our laboratory by CGH (20, 26, 29). (*ii*) High-level copy-number increases (amplifications), which were frequently observed on single chromosomal bands in the above-mentioned tumors, were rare in these cervical carcinomas. This is consistent with data reported in the literature (22, 30, 31).

Summarizing the data from this study, we conclude that the sequence of genetic events that result in the transition of normal cervical epithelium to dysplasias and finally invasive carcinomas consists of the following steps. (*i*) Tetraploidization is the first genetic abnormality and occurs as early as in mildly dysplastic regions (17). The proliferative activity, determined by MIB-1 staining, is elevated (and increases during progression). HPV sequences were detected in one of the three successfully analyzed moderately dysplastic lesions. (*ii*) Severe dysplasias/CIS are almost invariably infected with high-risk HPV types. The tetraploidization as determined by DNA content measurements persists; however, the cells reveal a pronounced genomic instability indicated by scattered DNA histograms that extend to values as high as 8*c*. The gain or loss of specific chromosomes is not yet obvious. (*iii*) In addition to high-risk HPV infection, aneuploidy, and high proliferative activity, the specific gain of chromosome 3q sequences is the

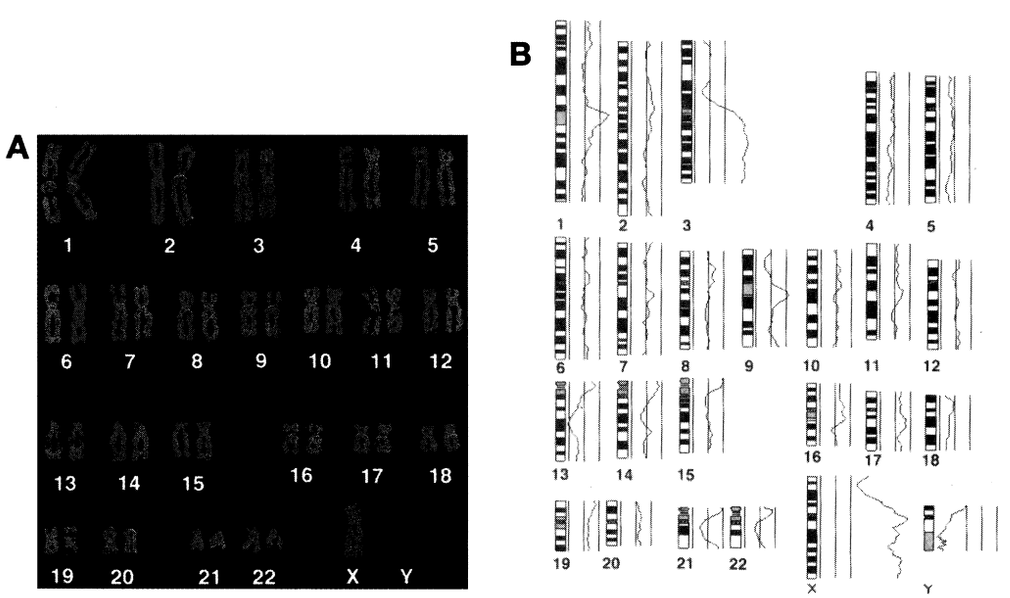

FIG. 3. (*A*) Display of a ratio image after CGH of an invasive carcinoma (case 3). A three-color look-up table was chosen for the visualization of fluorescein/rhodamine ratios: blue, balance between fluorescein and rhodamine values; green, overrepresentation of DNA in the tumor genome; red, loss of tumor DNA at the corresponding sequences. The chromosomes are ordered in a karyogram-like fashion. Note the consistency of the hybridization pattern on the homologous chromosomes. Chromosome 3q is gained and chromosomal band 13q21 is lost in this carcinoma. (*B*) CGH experiment with DNA extracted from the invasive carcinoma shown in *A*. The average ratio profile was used to identify chromosomal gains and losses in all cases. The three vertical lines on the right side of the chromosome ideograms represent different values of the fluorescence ratio between the tumor DNA and the normal DNA. The values are 0.75, 1, and 1.25 from left to right, respectively. The ratio profile (curve) was computed as a mean value of seven metaphase spreads. The ratio profile was in the normal range except for chromosome 3q (gain) and 13q21 (loss).

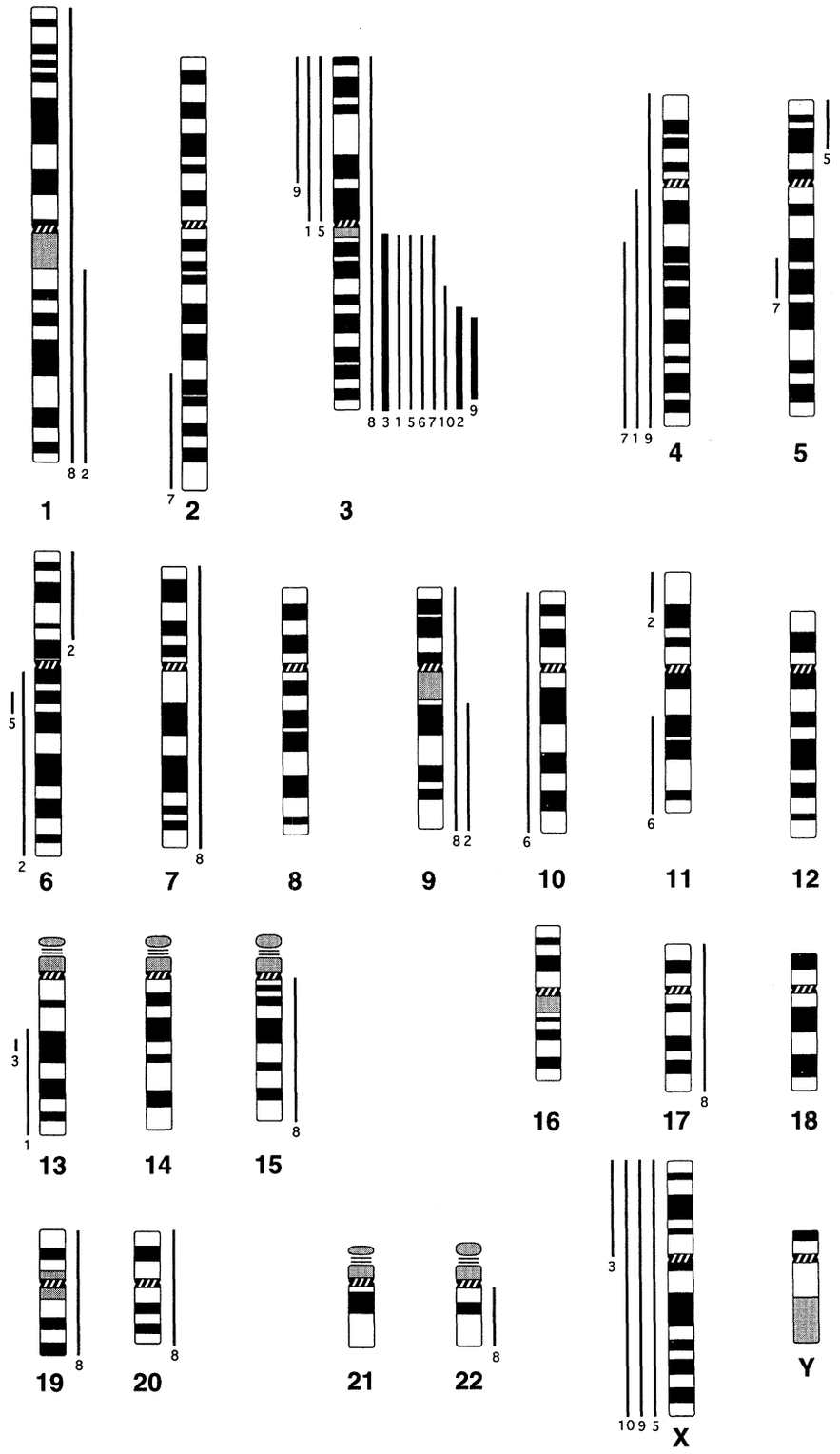

FIG. 4. Summary of the genetic imbalances detected in 10 primary invasive cervical carcinomas. Vertical lines on the left side of each chromosome ideogram represent loss of genetic material in the tumor, whereas those on the right side correspond to a gain. Changes in individual cases can be identified by the case number provided at the bottom of each line. High-level copy-number increases are represented as solid bars. The long arm of chromosome 3 was overrepresented in 9 of 10 cases. The consensus region on 3q that is gained in the carcinomas extends from band 3q24 to band 3q28.

most consistent chromosomal aberration that becomes detectable when severely dysplastic cells have progressed to invasive cervical carcinomas (stage T1).

Interphase fluorescence *in situ* hybridization with 3q probes on tissue sections will allow quantification of the cells that actually carry the gain of 3q and to determine their cellular origin. Whether the gain of chromosome 3q is a useful genetic marker to predict the risk of progression in severe dysplasias/CIS can now be investigated by using interphase fluorescence *in situ* hybridization directly on routine cytological preparations.

We thank Ulla Aspenblad, Uwe Köster, Richard Daniel, and Kelly Just for excellent technical assistance and Gabi Green for critically reading the manuscript. This study was supported in part by the Flensburger Tumorarchiv, e.V., the Swedish Cancer Society, and the Cancer Society in Stockholm, Sweden. E.S. received a fellowship from the Deutsche Forschungsgemeinschaft.

1. Foulds, L. (1958) *J. Chronic Dis.* **8,** 2–37.
2. Nowell, P. C. (1976) *Science* **194,** 23–28.
3. Klein, G. & Klein, E. (1985) *Nature (London)* **315,** 190–195.
4. Bishop, J. M. (1991) *Cell* **64,** 235–248.

5. Fearon, E. & Vogelstein, B. (1990) *Cell* **61,** 759–767.
6. zur Hausen, H. (1989) in *Advances in Viral Oncology*, ed. Klein, G. (Raven, New York), Vol. 8, pp. 1–26.
7. Bosch, F. X., Manos, M. M., Munoz, N., Sherman, M., Jansen, A. M., Peto, J., Schiffman, M. H., Moreno, V., Kurman, R. & Shah, K. V. (1995) *J. Natl. Cancer Inst.* **87,** 796–802.
8. Hildesheim, A., Schiffman, M. H., Gravitt, P. E., Glass, A. G., Greer, C. E., Zhang, T., Scott, D. R., Rush, B. B., Lawler, P., Sherman, M. E., Hurman, R. J. & Manos, M. M. (1994) *J. Infect. Dis.* **169,** 235–240.
9. zur Hausen, H. (1994) *Lancet* **343,** 955–957.
10. Granberg, I. (1971) *Hereditas* **68,** 165–218.
11. Atkin, N. B., Baker, M. C. & Fox, M. F. (1990) *Cancer Genet. Cytogenet.* **44,** 229–241.
12. Popescu, C. N. & DiPaolo, J. A. (1992) *Cancer Genet. Cytogenet.* **60,** 214–215.
13. Kallioniemi, A., Kallioniemi, O.-P., Sudar, D., Rutovitz, D., Gray, J. W., Waldman, F. & Pinkel, D. (1992) *Science* **258,** 818–821.
14. Du Manoir, S., Speicher, M. R., Joos, S., Schröck, E., Popp, S., Döhner, H., Kovacs, G., Robert-Nicoud, M., Lichter, P. & Cremer, T. (1993) *Hum. Genet.* **90,** 590–610.
15. Speicher, M. R., du Manoir, S., Schröck, E., Holtgreve-Grez, H., Schoell, B., Lengauer, C., Cremer, T. & Ried, T. (1993) *Hum. Mol. Genet.* **2,** 1907–1914.
16. Poulsen, H. E., Taylor, C. W. & Sobin, L. H. (1975) *WHO International Histological Classification of Tumors*, No. 13 (WHO, Geneva).
17. Steinbeck, R. G., Heselmeyer, K. M., Moberger, H. B. & Auer, G. U. (1995) *Acta Oncol.* **34,** 171–175.
18. Auer, G., Askensten, U. & Ahrens, O. (1989) *Hum. Pathol.* **20,** 518–527.
19. Manos, M. M., Ting, Y., Wright, D. K., Lewis, A. J., Broker, T. R. & Wolinsky, S. M. (1989) *Molecular Diagnostics of Human Cancer: Cancer Cells*, eds. Furth, M. & Greaves, M. (Cold Spring Harbor Lab. Press, Plainview, NY), Vol. 7, p. 209.
20. Ried, T., Just, K. E., Holtgreve-Grez, H., du Manoir, S., Speicher, M. R., Schröck, E., Latham, C., Blegen, H., Zetterberg, A., Cremer, T. & Auer, G. (1995) *Cancer Res.* **55,** 5415–5423.
21. Du Manoir, S., Schröck, E., Bentz, M., Speicher, M. R., Joos, S., Ried, T., Lichter, P. & Cremer, T. (1995) *Cytometry* **19,** 27–41.
22. Yokota, J., Tsukada, Y., Nakajima, T., Gotoh, M., Shimosato, Y., Mori, N., Tsunokawo, Y., Sugimura, T. & Terada, M. (1989) *Cancer Res.* **49,** 3598–3601.
23. Srivatsan, E. S., Misra, B. C., Venugopalan, M. & Wilczynski, S. P. (1991) *Am. J. Hum. Genet.* **49,** 868–877.
24. Hampton, G. M., Penny, L. A., Baergen, R. N., Larson, A., Brewer, C., Liao, S., Busby-Earle, R. M. C., Williams, A. W. R., Steel, C. M., Bird, C. C., Stanbridge, E. J. & Evans, G. A. (1994) *Proc. Natl. Acad. Sci. USA* **91,** 6953–6957.
25. Jesudasan, R. A., Rahman, R. A., Chandrashekharappa, S., Evans, G. A. & Srivatsan, E. S. (1995) *Am. J. Hum. Genet.* **56,** 705–715.
26. Ried, T., Petersen, I., Holtgreve-Grez, H., Speicher, M. R., Schröck, E., du Manoir, S. & Cremer, T. (1994) *Cancer Res.* **54,** 1801–1806.
27. Dyson, N., Howley, P. M., Münger, K. & Harlow, E. (1989) *Science* **243,** 934–937.
28. Scheffner, M., Werness, B. A., Huibregtse, J. M., Levine, A. J. & Howley, P. M. (1990) *Cell* **63,** 1129–1136.
29. Schröck, E., Thiel, G., Lozanova, T., du Manoir, S., Meffert, M. C., Jauch, A., Speicher, M. R., Nürnberg, P., Vogel, S., Jänisch, W., Donis-Keller, H., Ried, T., Witkowski, R. & Cremer, T. (1994) *Am. J. Pathol.* **144,** 1203–1218.
30. Oka, K., Nakano, T. & Arai, T. (1993) *Cancer* **73,** 668–671.
31. Mitra, A. B., Murty, V. V. V. S., Pratap, M., Sodhani, P. & Chaganti, R. S. K. (1994) *Cancer Res.* **54,** 637–639.